Coherent optical association of a single molecule

Yichao Yu,[1,2,3,*] Kenneth Wang,[1,2,3] Jonathan D. Hood,[4] Lewis R. B. Picard,[1,2,3] Jessie T. Zhang,[1,2,3] William B. Cairncross,[2,1,3] Jeremy M. Hutson,[5] Till Rosenband,[1] and Kang-Kuen Ni[2,1,3,†]

[1] *Department of Physics, Harvard University, Cambridge, Massachusetts 02138, USA*
[2] *Department of Chemistry and Chemical Biology, Harvard University, Cambridge, Massachusetts 02138, USA*
[3] *Harvard-MIT Center for Ultracold Atoms, Cambridge, Massachusetts 02138, USA*
[4] *Department of Chemistry, Purdue University, West Lafayette, Indianna, 47906*
[5] *Joint Quantum Centre Durham-Newcastle, Department of Chemistry, Durham University, Durham, DH1 3LE, United Kingdom*

(Dated: October 15, 2020)

We report on coherent association of a single weakly-bound NaCs molecule in an optical tweezer through an optical Raman transition without the use of a Feshbach resonance. Our scheme borrows transition dipole moment while reducing photon scattering by selecting a deeply bound electronic excited intermediate state. Starting from two atoms in their relative motional ground state, we achieve optical transfer efficiency of 69%. The molecule has a binding energy of 770.200516(24)MHz at 8.8 G and lifetime up to 1ms (1 ms seems long here) with more than 60% of the molecule created in the motional ground state. This technique is general without relying on narrow excited state lines or Feshbach resonances and could allow a wider range of molecular species to be assembled atom-by-atom.

Diverse species of fully quantum controlled ultracold molecules are desired for a wide variety of applications including precision measurements [1], quantum simulations [2], quantum information processing [3, 4], and studies of ultracold chemistry [5–7]. While many innovative approaches demonstrated in the last few years have directly cooled different species of diatomic or polyatomic molecules below 1 mK [8, 9], the coldest and the highest phase-space-density gas to date in an ensemble [10] or as individuals [11] have been achieved through the association of ultracold atoms.

Such ultracold molecular association takes advantage of the much developed cooling and trapping techniques for atoms as a starting point. To overcome the challenges of small wavefunction overlap and the large release of binding energy of converting atoms to deeply-bound molecules, a two-step approach has been established to first associate atom pairs into weakly-bound molecules, and then transfer the molecules from this single internal state to a desired rovibrational and electronic state [12–20]. So far, all of such association processes utilized a magnetic Feshbach scattering resonance and have been applied to bialkali molecules. The only exception is Sr_2 where narrow linewidth excited states are available and optical association can be driven coherently [21, 22]. The requirement of a Feshbach resonance to enhance atom-to-molecule wavefunction overlap or the existence of narrow excited state lines limits the generality of the association technique.

Here, we demonstrate coherent association of an atom pair to a weakly bound molecule using a two-photon optical Raman transfer via an electronic excited state, schematically shown in Fig. 1A, neither using a Feshbach resonance nor a narrow excited state. The resulting single molecule is in a single internal quantum state and predominately in its motional ground state. Our scheme is based on a choice of vibrational state of the electronic excited state $c^3\Sigma^+(\Omega = 1)$ that has the theoretical best raman Rabi frequency to photon scattering ratio. To further increase this ratio and reduce technical requirements such as intensity stability, we choose an initial and final state where the matrix elements with the excited state are as balanced as possible. This approach minimizes the reliance on system specific properties and could therefore be applied to creating other molecular species or larger molecules atom-by-atom with full quantum state control.

The essence of an optical Raman transfer can be illustrated using a three-level system (Fig. 1A), where the initial atomic state, the target weakly-bound molecular state are coupled to an excited intermediate state by two photons, Ω_a and Ω_m, with one-photon detuning Δ, and two-photon detuning, δ. The transfer Raman Rabi Rate, $\Omega_a\Omega_m/2\Delta$, is accompanied by a photon scattering rate which is a sum of all coupling sources $\Gamma_e\Omega^2/4\Delta^2$, where Γ_e is the excited state linewidth [23]. Unlike for Raman transitions in atoms, the two matrix elements here, Ω_m and Ω_a, are greatly imbalanced due to the small wavefunction overlap between the atomic state and the excited molecular state, and the scattering is predominantly from the molecular state. Furthermore, the energy difference between the atomic and weakly bound state is small (< 1GHz) compared to the single photon detuning, Δ, so the molecular state can scatter off both beams at roughly the same single photon detuning. Thus, the scattering is given by $\Gamma_e\Omega_m^2/2\Delta^2$ [24]. The ratio between the Raman Rabi frequency and the scattering rate, $\Omega_a/\Omega_m \times \Delta/\Gamma_e$, depends on the ratio of the two matrix elements and how far detuned the laser is from the transition in units of the linewidth. To ensure a coherent process, a detuning as large as possible, while maintaining a realistic Raman

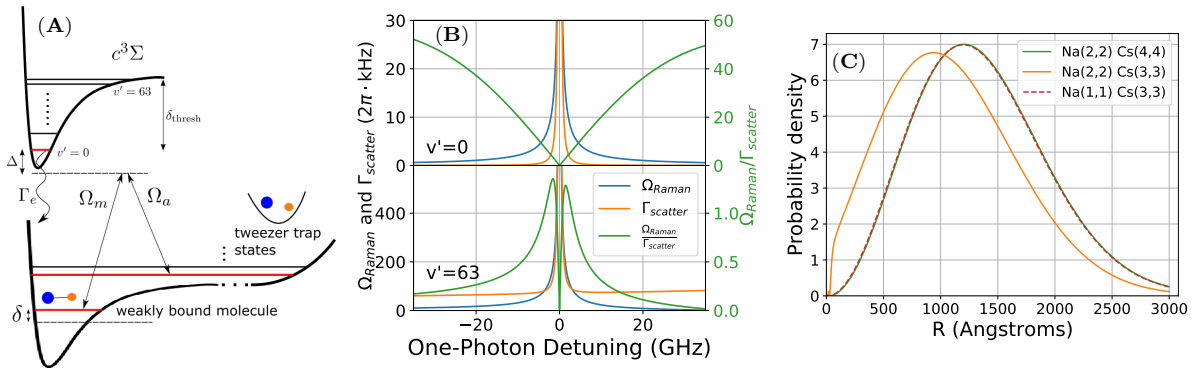

FIG. 1. Optical creation of single molecule from single atoms in tweezer. (A) Schematics of the optical transition from an atom pair to a weakly bound molecule. The initial state is the relative motional ground state between the two atoms and the final state is the first molecular bound state. The transition is driven by a pair of laser frequencies matching the binding energy of the molecule. The lasers are detuned from an excited molecular state in the $c^3\Sigma$ potential by Δ in order to suppress the scattering during the transfer. (B) Comparison between using a weakly bound and a deeply bound excited state as intermediate state for the Raman transition. The deeply bound excited state (upper half $v'=0$) has a smaller Raman Rabi frequency (Ω_{Raman}) compared to the weakly bound excited state (lower half $v'=63$) at a given detuning. However, the scattering rate ($\Gamma_{scatter}$) is also much lower, which results in a larger Raman Rabi frequency to scattering rate ratio. (C) Enhancement of short range wavefunction. The large scattering length for the $Na(2,2), Cs(3,3)$ state creates an interaction shift comparable to the axial trapping frequency. This causes a significant change in the relative wavefunction especially at short intranuclear distance (R). Compared to other spin states with weaker interaction, the wavefunction at short distance ($R < 100$Å) is significantly enhanced.

Rabi frequency, is preferred. With the multiple excited vibrational states present in a molecular potential, the total scattering rate and Raman Rabi rate become a sum over the scattering rates and Raman Rabi rates of the individual states.

Pioneering experiments used weakly bound molecular excited states in the Raman transition to ensure a large Raman Rabi frequency [25, 26]. However, such choice of state suffers from strong scattering of the nearby atomic excited state to render it incoherent, resulting in molecule loss. This scattering is proportional to $1/\delta^2_{thresh}$, where δ_{thresh} is the detuning from the dissociation threshold, and thus can be made smaller by detuning away from the dissociation threshold.

To find the optimal excited intermediate state, we perform a calculation of the Raman Rabi frequency and scattering rate at different detunings from the atomic threshold taking into account of all states of the $c^3\Sigma^+(\Omega=1)$ excited molecular state potential (full result in SM) [27, 28]. As shown in Fig. 1B, the ratio of the Raman Rabi rate to scattering rate can be made larger for more deeply bound states compared to weakly bound states at a cost of a smaller Raman Rabi frequency. As a result, we choose a deeply bound molecular excited state ($v'=0$ of $c^3\Sigma^+(\Omega=1)$) as an intermediate state to drive the Raman transition.

As previously discussed, the ratio of the Raman Rabi rate to the scattering rate is proportional to the Ω_a/Ω_m ratio. The smaller this ratio is, the farther the laser needs to be detuned to achieve the same Raman Rabi rate to scattering rate ratio, which lowers the Raman Rabi rate. In addition to reducing how far the laser needs to be detuned from the transition, a larger Ω_a/Ω_m ratio also relaxes the intensity stability requirement, a key potential technical limitation. The position of the two photon resonance depends on the laser power predominantly through the AC Stark shift on the molecular state, $\Omega_m^2/2\Delta$ [29]. The ratio of the AC Stark shift to the Raman Rabi frequency is Ω_m/Ω_a, Thus, the laser intensity needs to be stabilized to better than the inverse of this ratio to fluctuate by less than a linewidth in a coherent process. The ratio, Ω_a/Ω_m can be changed through the choice of initial and final states. In particular, it can be made larger by increasing the coupling of the atomic state with the excited molecular state. Due to the small size of the molecular wavefunction, the coupling between the ground atomic state and the excited molecular state is approximately proportional to the value of the relative atomic wavefunction at short distance within the molecular potential. In addition to the confinement, this value is related to the interaction between the two atoms. For states with a large scattering length (positive or negative), the phase shift in the relative wavefunction between the atoms can significantly increase the short range wavefunction (Fig. 1C). The increase in the coupling is proportional to (quote/cite Olive's equation?). For our system, we denote the possible hyperfine states of the atoms as $|\uparrow_{\text{Cs}}\rangle = |F=4, m_F=4\rangle_{\text{Cs}}$, $|\downarrow_{\text{Cs}}\rangle = |F=3, m_F=3\rangle_{\text{Cs}}$, $|\uparrow_{\text{Na}}\rangle = |F=2, m_F=2\rangle_{\text{Na}}$, and $|\downarrow_{\text{Na}}\rangle = |F=1, m_F=1\rangle_{\text{Na}}$. Among the stable spin combinations, $|\uparrow_{\text{Na}}\uparrow_{\text{Cs}}\rangle$ and $|\downarrow_{\text{Na}}\downarrow_{\text{Cs}}\rangle$ both have small scattering lengths of $30.4a_0$, and $13.7a_0$ respectively, but the

$|\uparrow_{\mathrm{Na}}\downarrow_{\mathrm{Cs}}\rangle$ combination has a large and negative scattering length of $a(\uparrow_{\mathrm{Na}}\downarrow_{\mathrm{Cs}}) = -693.8a_0$ (interaction shift $\approx$ binding?) [30]. In addition to the increased atomic coupling, Ω_a, with the $|\uparrow_{\mathrm{Na}}\downarrow_{\mathrm{Cs}}\rangle$ hyperfine combination, coupled channel calculations show that the most weakly bound molecular state that is predominantly in this spin combination also has reduced coupling, Ω_m, with the excited state when compared with the $|\uparrow_{\mathrm{Na}}\uparrow_{\mathrm{Cs}}\rangle$ and $|\downarrow_{\mathrm{Na}}\downarrow_{\mathrm{Cs}}\rangle$ bound states. Therefore, using an initial $|\uparrow_{\mathrm{Na}}\downarrow_{\mathrm{Cs}}\rangle$ hyperfine combination results in a Ω_a/Ω_m ratio of about 0.05 instead of a ratio of about 0.003 with the other combinations. Thus, we choose the $|\uparrow_{\mathrm{Na}}\downarrow_{\mathrm{Cs}}\rangle$ spin combination as our initial state and drive to the first bound state for the $|\uparrow_{\mathrm{Na}}\downarrow_{\mathrm{Cs}}\rangle$ spin combination.

To perform the Raman transfer, we use our apparatus described in our previous work [31]. Our experiment begins by stochastically loading a single ^{23}Na atom and a single ^{133}Cs atom into an optical tweezer from a dual-species MOT into separate optical tweezers. The atoms are initially imaged to distinguish between loading of two atoms, one atom (Na or Cs), or no atom in order to perform post selection. We then perform simultaneous Raman sideband cooling (RSC) to cool both atoms into the 3-dimensional motional ground state of their optical tweezers. After RSC, the Na tweezer is moved by sweeping the frequency on an acoustical optical beam deflector (AOBD) to overlap with the Cs tweezer before smoothly ramping off, so that the Na and Cs atoms are merged into the same tweezer [31]. The spin states for the Na and Cs atoms after RSC and during the merge process are $|\uparrow_{\mathrm{Na}}\uparrow_{\mathrm{Cs}}\rangle$. This states combination has a low scattering length, which allows the two atoms to be merged into the same tweezer with minimum pertubation on each other and thus they remain in the motional ground state after the merge.

After preparing the Na and Cs atoms in the same tweezer in a single quantum state, we need to drive the atoms into the large scattering length $|\uparrow_{\mathrm{Na}}\downarrow_{\mathrm{Cs}}\rangle$ hyperfine combination. To do this, we perform a spin flip taking into account the interaction shift [30] using a Cs Raman transition to drive the Cs atom into the $|\downarrow_{\mathrm{Cs}}\rangle$ state. The new spin state combination has a larger scattering length of $-693.8a_0$ which generates a interaction shift of $-30.7kHz$ in the tweezer. This interaction shift is larger than the differential axial trapping frequency between Na and Cs atoms, which decouples the relative and center of mass motional state and improves the robustness of our preparation of the relative motion ground state.

After the atoms are prepared in the $|\uparrow_{\mathrm{Na}}\uparrow_{\mathrm{Cs}}\rangle$ hyperfine combination, we then perform the Raman transfer. The pulse sequence for this step is shown in Fig. 2B. Instead of adding another beam to drive the Raman transition on the atoms in the tweezer, we use the tweezer itself to achieve this goal. In particular, we turn on two co-propagating frequencies in the tweezer during the Raman pulse. The dual use of the tweezer beam ensures that there is not any undesired laser frequency that can interfere with the Raman transition, and also allows us to maximize the Raman Rabi frequency and minimize the transfer time. After the total tweezer power is set to the desired value, we smoothly ramp down the power of one frequency in the tweezer while simultaneously ramping up the power of a different frequency so that the total tweezer power remains unchanged. Both frequencies are kept on for a variable length of time before the process is reversed and we return to having a single frequency in the tweezer. In addition to reducing the number of laser beams during the Raman transition, we also found the spectral purity of the laser to be critical for achieving a higher transfer efficiency. The tweezer and Raman beams are generated by amplifying a 1037nm external cavity diode laser (ECDL) with a fiber amplifier, which produces a broad band amplified spontaneous emission (ASE) in addition to the desired frequency. This increases the scattering rate due to coupling to other excited states. We use a Bragg grating with a line width (FWHM) of 50GHz to clean up the laser spectrum and found it reduces the scattering rate by at least a factor of 2 for a particular single photon detuning.

Guided by coupled channel calculations, we locate the Raman resonance for the atom to molecule transition at 770.59430(17)MHz (Fig. 2C) with a $15mW$ tweezer at $288560GHz$ which corresponds to a $145GHz$ single photon detuning. (We can maybe add information about the prediction here?) The background level of 31% corresponds to the probability of preparing the two atoms in the relative motional ground state. When the atoms are transferred into the molecule state by the Raman transition, there is a decrease in the two body survival since the resulting molecule is not directly detected by our imaging step. We observed the narrowest linewidth of 7.56(82)kHz for the Raman resonance at a pulse time of 0.12ms, which corresponds to a linewidth-pulsetime product of 0.907(98). This is consistent with the expected value of 0.80 for an ideal π pulse which is an evidence that the transfer is coherent. In order to verify the coherence of the transfer directly, we fix the Raman frequency on resonance and scan the pulse time. Fig. 2D shows the observed Rabi oscillation between the atomic and molecular states. Fitting the data with a decaying Rabi oscillation suggests that 69% of initial ground state atoms are transferred into the molecular state.

In order to understand the fidelity of molecule formation, we fit our measurements to a model that includes a Raman Rabi frequency and a finite lifetime for the final molecular state (Fig. 3A). We account for the effect of atomic state loss by measuring the single and two body lifetime of the atoms directly (Fig. 3B). The fit shows that we have a Raman Rabi frequency of $2\pi\times3.282(42)$kHz. The molecule we form has a lifetime of 0.204(13)ms which is the main limitation on the fidelity of the transfer. The molecule lifetime can be verified

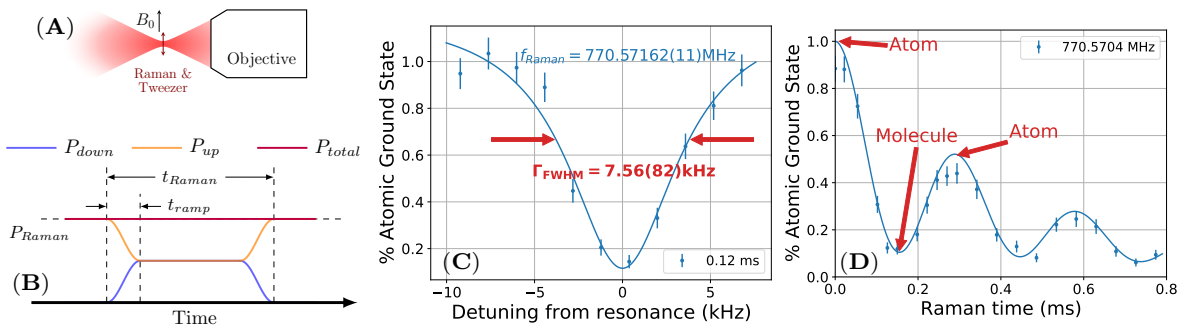

FIG. 2. (A) Geometry and polarization of trap and Raman beam relative to the bias magnetic field. The tweezer and Raman beam is focused through an objective to define the location of the atoms and molecule. We use a bias B field of $B_0 = 8.8G$ alone the tweezer polarization to define the quantization axis. As a result, the atoms experiences predominately π polarization from the tweezer. (B) Molecule formation pulse sequence. The tweezer initially consists of only up leg power. When driving the Raman transition, the up leg power is smoothly ramped down and the down leg power ramped up over $10\mu s$ while maintaining the total power of the tweezer. This minimizes the heating on the atoms due to power fluctuation while maximizes the time with maximum Raman Rabi frequency when the up and down leg powers are equal. (C) Raman resonance from atomic state $Na(2,2)$ $Cs(3,3)$ to the first molecular bound state using a 0.12ms pulse. The full width half maximum (FWHM) of 7.56(82)kHz of the resonance is consistent with the FWHM for a coherent 0.12ms π pulse 6.7kHz. (D) Raman pulse time scan on resonance. A decaying Rabi oscillation can be observed proving the coherence of the Raman transfer process.

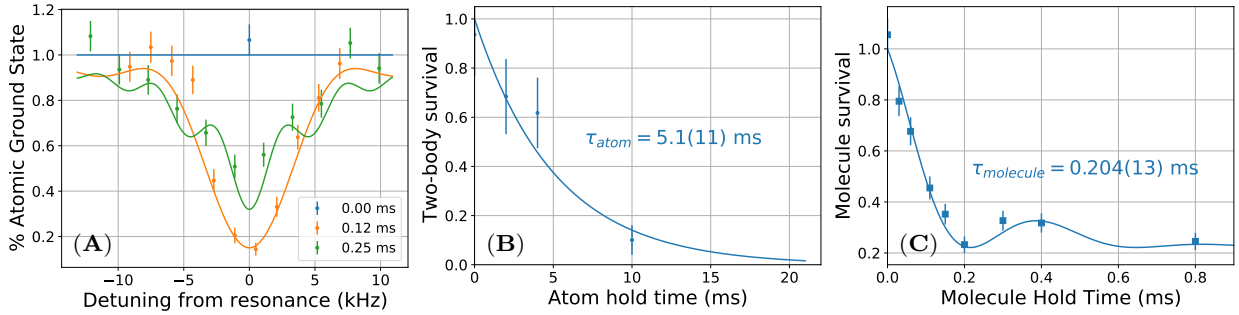

FIG. 3. (A) Fitting of Raman detuning scans at different times to a model of Raman transition with loss on the atom and molecule state. The combined fit is used to determine both the Raman Rabi frequency and the loss rates. (B) Two-body atom lifetime in 15mW of trap depth caused by off-resonance photoassociation. This is used to improve the fitting of the Raman transfer data. (C) Direct measurement of molecule lifetime in 15mW of trap depth. Molecule survival is detected by dissociating back to atoms using a second Raman transition. The lifetime is consistent with the 0.204(13)ms measured from the Raman transition data. The oscillation in the survival is the result of the interference between the two Raman pulses with incomplete transfer.

directly by adding a second Raman pulse to dissociate the molecule back to atoms after a variable wait time (Fig. 3C). The result shows a molecular lifetime consistent with our fitting of the decaying Rabi oscillation.

The ratio of molecule scattering rate to the Rabi frequency is larger than the theory prediction by more than a factor of 10. Based on the calculation above, if this comes from the coupling to the $v' = 0$ excited state, it can be either due to a high ratio of Ω_m/Ω_a or a large Γ_e. Additionally, coupling to other excited states can also add an offset to both the Raman Rabi frequency and the scattering rate which can affect the scattering rate to Rabi frequency ratio.

In order to verify whether any one of these known sources are the origin of the discrepancy, we measured the Raman resonance as a function of the tweezer power and single photon frequency. The important results from the fits are the 2 photon resonance frequency (light shift), Raman Rabi frequency, atomic lifetime and molecular lifetime. Each of these quantities provide us with information about a different combination of physical processes and the detuning dependency of them allows us to distinguish the contribution from the $v' = 0$ excited states and other states.

First we look at the change in resonance frequency. As a function of the tweezer power, we observe a linear dependency on the resonance frequency caused by the differential light shift between the atomic and molecu-

lar state (Fig. 4A). When we vary the tweezer frequency around the $v' = 0$ excited state, we can further observe a $1/\delta$ component and a constant component in the experimentally explored region. The background is caused by coupling to other excited states that are further away in energy. The $1/\Delta$ component, however, is predominantly due to the coupling between the molecular state and the $v' = 0$ excited state. From this measurement, we can calculate a matrix element between the molecular state and the excited state, Ω_m, of $2\pi \times 36.162(20)\text{MHz}/\sqrt{\text{mW}}$ or $2\pi \times 140.056(78)$MHz for the 15mW tweezer power used above. This number is consistent with the value of $2\pi \times 27\text{MHz}/\sqrt{\text{mW}}$ calculated from theory.

In order to calculate the matrix element ratio, we now need to extract the matrix element between the atomic state and the excited molecular state, Ω_a. We do this by measuring the dependencies of the Raman Rabi frequency, which depends on both Ω_m and Ω_a. The Raman Rabi frequency shows a non-linear dependency on the tweezer power due to the change in the atomic wavefunction caused by the change in confinement (Fig. 4B). The atomic matrix element, Ω_a, is proportional to the the short range atomic wavefunction amplitude, which scales as $P^{0.375}$ for weakly interacting particles. However, due to the strong interaction between the two atoms, this approximation breaks down. Instead, theory calculation shows that the scaling is very well approximated by $P^{0.29}$ within the range of confinement in our experiment. Combined with the intensity factor, the Raman Rabi frequency should scale with $P^{1.29}$, which agrees with our experimental result. Similar to the light shift, there is also an offset and a $v' = 0$ component in the Raman Rabi frequency that scales as $1/\Delta$. The $v' = 0$ component of the Raman Rabi frequency is $2\pi \times 161.8(22)\text{Hz} \cdot \text{mW}^{-1.29}$, or $2\pi \times 5.324(73)$kHz at 15mW tweezer power. Together with the Ω_m measured above, the up leg Rabi frequency is $2\pi \times 11.53(16)$MHz. This gives a Rabi frequency, and therefore matrix element, ratio of 12.14(16), which is in fact better than the theory prediction of 23.7 and should not cause the scattering from the $v' = 0$ state to be higher than expected.

Unfortunately, the offset in the Raman Rabi frequency fit cancels the Rabi frequency for red detuning Raman transition and reduces it by about 30% at the current detuning. However, this difference is not enough to explain the difference we observed in the experiment. The same offset will increase the Rabi frequency for blue detuning but we have observed additional excited states at slightly higher frequencies which prevent the blue side of the transition to be usable for the Raman transition.

Based on our previous measurements of the excited state using photoassociation (PA) spectroscopy, the natural linewidth of the $v' = 0$ excited state is no larger than 20MHz. This suggests that the excited state linewidth should not cause a stronger than expected scattering from $v' = 0$ state either.

These results suggests that the decoherence or loss we observed during the the Raman transition comes from either a higher than expected background scattering rate or a different intrinsic or technical source that we have not accounted for. As mentioned above, we have observed significant improvment in the coherence time by filtering out most of the ASE from the laser suggesting the spectral purity of the laser is a significant source of scattering. Although we have good control on the total power of the tweezer and Raman beam to stabilize the light shift on the transition, the power ratio of the two frequencies within the beam is not yet controlled as tightly and may result in a residual resonance fluctuation. Finally, Fig. 4C shows the two-body scattering rate for the atomic initial state. The scattering rate scales as $P_{tweezer}^{2.58}$ which is inconsistent with the prediction based on single photon scattering process. Although the absolute scattering rate is much lower than the total decoherence rate and we have not been able to observe a dependency on the detuning in order to verify if the scattering process is related to the $v' = 0$ state, the power scaling strongly suggests the existence of a unknown two photon scattering process.

B field dependency $42.17(24)kHz/G$ which agrees with theory prediction of $...kHz/G$.

In conclusion, we have formed a weakly bound NaCs molecule in an optical tweezer via an optical Raman transfer. A theoretical investigation including all excited states of $c^3\Sigma^+(\Omega = 1)$ and coupled channel ground state wavefunctions indicated better transfer efficiency using a deeply bound intermediate state and the $|\uparrow_{\text{Na}}\downarrow_{\text{Cs}}\rangle$ hyperfine state combination. Using these theoretical insights, we located the weakly bound state and coherently associated the atoms into the weakly bound molecule. Our transfer efficiency is limited by an unknown scattering source resulting in measured scattering rates over 10 times larger than theory predictions. Despite this limitation, the transfer efficiency may be further improved by increasing the Ω_a/Ω_m ratio by exploring the possibility of driving to more deeply bound states. There may also be a better choice of single photon detuning to increase the Raman Rabi frequency, since our location results in about 30% cancellation of the Raman Rabi frequency due to an offset of unknown origin. (Do we want to mention also technical improvements as another way to potentially improve our signal? Though I guess that was mentioned directly in the paragraph above...) Nevertheless, our technique, with the right choice of parameters, can be used to form a more diverse set of molecular species, since it does not rely on a magnetic Feshbach resonance or a narrow excited state (More sentences here to discuss scientific outlook, but without repeating the introduction...? Yes, on topics related to single molecules for exciting science!!)

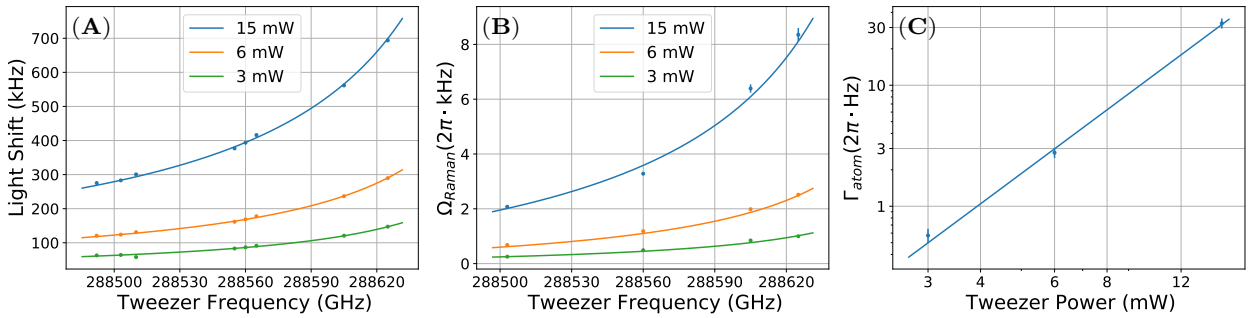

FIG. 4. Raman transition parameters as a function of tweezer and Raman power and detuning. (A) The light shift of the Raman resonance scales as $P_{tweezer}$ and follows $1/\Delta$ with an offset. The fit also includes a small term that is proportional to $P^2_{tweezer}$ which is caused by the effective magnetic field generated by the tweezer which is perpendicular to the real magnetic field. (B) Raman Rabi frequency scales as $P^{1.29}_{tweezer}$ and follows $1/\Delta$ with an offset. From these results we can confirm the theory prediction of the atom-molecule matrix element ratio. (C) Atomic scattering rate scales as $P^{2.58}_{tweezer}$, this is consistent with a two photon scattering process. We have not measured a clear dependency of the loss rate on the tweezer detuning.

* yichaoyu@g.harvard.edu
† ni@chemistry.harvard.edu

[1] I. Kozyryev and N. R. Hutzler, Physical Review Letters **119**, 133002 (2017), publisher: American Physical Society.
[2] N. Y. Yao, M. P. Zaletel, D. M. Stamper-Kurn, and A. Vishwanath, Nature Physics **14**, 405 (2018).
[3] D. DeMille, Phys. Rev. Lett. **88**, 067901 (2002).
[4] K.-K. Ni, T. Rosenband, and D. D. Grimes, Chem. Sci. **9**, 6830 (2018).
[5] J. L. Bohn, A. M. Rey, and J. Ye, Science **357**, 1002 (2017).
[6] N. Balakrishnan, J. Chem. Phys. **145**, 150901 (2016), http://dx.doi.org/10.1063/1.4964096.
[7] M.-G. Hu, Y. Liu, D. D. Grimes, Y.-W. Lin, A. H. Gheorghe, R. Vexiau, N. Bouloufa-Maafa, O. Dulieu, T. Rosenband, and K.-K. Ni, Science **366**, 1111 (2019), https://science.sciencemag.org/content/366/6469/1111.full.pdf.
[8] E. B. Norrgard, D. J. McCarron, M. H. Steinecker, M. R. Tarbutt, and D. DeMille, Phys. Rev. Lett. **116**, 063004 (2016).
[9] D. Mitra, N. B. Vilas, C. Hallas, L. Anderegg, B. L. Augenbraun, L. Baum, C. Miller, S. Raval, and J. M. Doyle, Science **369**, 1366 (2020), https://science.sciencemag.org/content/369/6509/1366.full.pdf.
[10] L. De Marco, G. Valtolina, K. Matsuda, W. G. Tobias, J. P. Covey, and J. Ye, arXiv preprint arXiv:1808.00028 (2018).
[11] J. T. Zhang, Y. Yu, W. B. Cairncross, K. Wang, L. R. B. Picard, J. D. Hood, Y.-W. Lin, J. M. Hutson, and K.-K. Ni, Phys. Rev. Lett. **124**, 253401 (2020).
[12] J. G. Danzl, E. Haller, M. Gustavsson, M. J. Mark, R. Hart, N. Bouloufa, O. Dulieu, H. Ritsch, and H.-C. Nägerl, Science **321**, 1062 (2008).
[13] K.-K. Ni, S. Ospelkaus, M. H. G. de Miranda, A. Pe'er, B. Neyenhuis, J. J. Zirbel, S. Kotochigova, P. S. Julienne, D. S. Jin, and J. Ye, Science **322**, 231 (2008).
[14] F. Lang, K. Winkler, C. Strauss, R. Grimm, and J. Hecker Denschlag, Phys. Rev. Lett. **101**, 133005 (2008).
[15] T. Takekoshi, L. Reichsöllner, A. Schindewolf, J. M. Hutson, C. R. Le Sueur, O. Dulieu, F. Ferlaino, R. Grimm, and H.-C. Nägerl, Phys. Rev. Lett. **113**, 205301 (2014).
[16] P. K. Molony, P. D. Gregory, Z. Ji, B. Lu, M. P. Köppinger, C. R. Le Sueur, C. L. Blackley, J. M. Hutson, and S. L. Cornish, Phys. Rev. Lett. **113**, 255301 (2014).
[17] J. W. Park, S. A. Will, and M. W. Zwierlein, Phys. Rev. Lett. **114**, 205302 (2015).
[18] M. Guo, B. Zhu, B. Lu, X. Ye, F. Wang, R. Vexiau, N. Bouloufa-Maafa, G. Quéméner, O. Dulieu, and D. Wang, Phys. Rev. Lett. **116**, 205303 (2016).
[19] S. S. Kondov, C.-H. Lee, K. H. Leung, C. Liedl, I. Majewska, R. Moszynski, and T. Zelevinsky, Nature Physics **15**, 1118–1122 (2019).
[20] K. K. Voges, P. Gersema, M. Meyer zum Alten Borgloh, T. A. Schulze, T. Hartmann, A. Zenesini, and S. Ospelkaus, Phys. Rev. Lett. **125**, 083401 (2020).
[21] G. Reinaudi, C. B. Osborn, M. McDonald, S. Kotochigova, and T. Zelevinsky, Phys. Rev. Lett. **109**, 115303 (2012).
[22] S. Stellmer, B. Pasquiou, R. Grimm, and F. Schreck, Phys. Rev. Lett. **109**, 115302 (2012).
[23] D. J. Wineland, M. Barrett, J. Britton, J. Chiaverini, B. DeMarco, W. M. Itano, B. Jelenković, C. Langer, D. Leibfried, V. Meyer, T. Rosenband, and T. Schätz, Philosophical Transactions of the Royal Society of London A: Mathematical, Physical and Engineering Sciences **361**, 1349 (2003), http://rsta.royalsocietypublishing.org/content/361/1808/1349.full.pd
[24] We choose the two beams to have equal power, which gives the highest Raman Rabi Rate at a fixed total power. Thus, this results in an additional factor of 2 coming from scattering off 2 beams.
[25] R. Wynar, R. S. Freeland, D. J. Han, C. Ryu, and D. J. Heinzen, Science **287**, 1016 (2000), http://science.sciencemag.org/content/287/5455/1016.full.pdf.
[26] T. Rom, T. Best, O. Mandel, A. Widera, M. Greiner, T. W. Hänsch, and I. Bloch, Phys. Rev. Lett. **93**, 073002 (2004).
[27] L. R. Liu, J. T. Zhang, Y. Yu, N. R. Hutzler, Y. Liu, T. Rosenband, and K.-K. Ni, arXiv:1701.03121 .

[28] A. Grochola, P. Kowalczyk, J. Szczepkowski, W. Jastrzebski, A. Wakim, P. Zabawa, and N. P. Bigelow, Phys. Rev. A **84**, 012507 (2011).
[29] There is an additional factor of 2 to account for the Stark shift of both beams.
[30] J. D. Hood, Y. Yu, Y.-W. Lin, J. T. Zhang, K. Wang, L. R. Liu, B. Gao, and K.-K. Ni, Phys. Rev. Research **2**, 023108 (2020).
[31] L. R. Liu, J. D. Hood, Y. Yu, J. T. Zhang, K. Wang, Y.-W. Lin, T. Rosenband, and K.-K. Ni, Phys. Rev. X **9**, 021039 (2019).